A NOVEL FREQUENCY SYNTHESIZER CONCEPT FOR WIRELESS COMMUNICATIONS

César Caballero Gaudes[1], *Mikko Valkama*[2], *Markku Renfors*[2]

[1] Grupo de Tecnologías de las Comunicaciones, CPS
Universidad de Zaragoza
María de Luna 1, 50018 Zaragoza, Spain

[2] Institute of Communications Engineering
Tampere University of Technology
P.O. Box 553, FIN-33101 Tampere, Finland

ABSTRACT

Strict requirements for high spectral purity, high operating frequencies and fast switching speed together with the power consumption limitations make the frequency synthesizer design an extremely challenging task for wireless applications. In this paper, a combination of analog and digital synthesis techniques is discussed and analyzed. A low frequency tone generated digitally is upconverted to the final frequency range by means of I/Q mixing. Ideally, the use of I/Q processing eliminates the need for any sideband suppression filtering. In practical implementations, however, the amplitudes and phases of the I and Q branches can only be matched with finite relative accuracy, resulting in finite image tone attenuation. Apart from I/Q imbalance, another practical non-ideality is the leakage of the local oscillator signals to the I/Q mixer output ports, creating another undesired tone at the synthesizer output. A compensation structure based on digital pre-distortion of the low frequency signals is presented to enhance the signal quality. Furthermore, a simple and practical algorithm for updating the compensator coefficients is proposed based on minimizing the envelope variation of the synthesizer output signal. Simulation results illustrate the performance of the proposed frequency synthesizer concept.

1. INTRODUCTION

In all the alternative architectures of radio transceivers, frequency synthesizers are needed in performing frequency translations. Oscillators generate sinusoidal waveforms used to shift baseband signals into upper frequencies and vice versa. Thus, the synthesis of high quality sinusoidal signals is one of the most critical functions of any wireless terminal. In general, the synthesizer has to be tunable across the wanted frequency band with tuning resolution equal to the channel spacing [1]-[4].

Several analog and digital design techniques are well-known by radio designers for generating sinusoidal waveforms [1]-[3]. Traditional analog synthesizer architectures are based on multiplying the frequency of a stable reference source using a phase-locked loop (PLL) with a frequency divider in the feedback path. In the basic schemes, the output frequency accuracy equals the reference accuracy and tuning is performed via a programmable divider [1][2]. In the previous years, there have been considerable efforts in order to replace the analog PLL based frequency synthesizers with their digital counterparts, mainly referred to as direct digital synthesis (DDS) [3]. Digital synthesis techniques generate samples of sine wave at the desired frequency, after which the samples are converted to analog domain by a digital-to-analog converter (DAC). So far digital techniques alone are unable to support sufficiently high frequency range with reasonable power dissipation. However, low phase noise, high resolution, and fast frequency switching have made DDS a promising approach in RF design [3][5].

This paper is organized as follows. In Section 2, the architecture of the proposed frequency synthesizer based on digital tuning and I/Q signal processing is presented. Then, in Section 3, the effects of I/Q mismatch and carrier leakage on the synthesizer output signal are analyzed and a digital pre-compensation scheme is proposed. With emphasis on implementation simplicity, an iterative coefficient update algorithm is also presented. In section 4, computer simulations are used to evaluate the performance of the proposed synthesis technique and some practical aspects are discussed in Section 5. Finally, conclusions are drawn in Section 6.

2. FREQUENCY SYNTHESIZER ARCHITECTURE

The current trend in frequency synthesizer design is focused towards architectures with higher (typically GHz) operating frequencies and faster tuning. Also of great concern are practical matters such as spurious response rejection, power consumption and integrability [1]-[4]. To achieve these objectives, the basic approach here is to use I/Q modulation to translate a digitally synthesized tunable low frequency tone to the final frequency range. The basic block diagram of the synthesizer is illustrated in Figure 1. Using I/Q mixing, the problem of sideband suppression is basically solved without demanding radio frequency filtering. All the tuning can be made in the digital part and the local oscillator (LO) frequency can be fixed in the mixing stage, thus facilitating the LO design. In addition, the digitally synthesized frequency range can be kept at a relative low level (ultimately within ± half the desired tuning width) resulting in feasible requirements for D/A converters and reasonable power consumption.

Practical implementations suffer from several non-idealities diminishing the spectral purity of the synthesized signal. Although the limitation in the number of bits used in the digital part produces spurious terms in the D/A converter outputs (and thus also in the actual synthesizer output), several DDS architectures have been reported with excellent spurious response [3]. More challenging problem in this context are the non-idealities introduced in the analog part. First of all, unavoidable gain and phase imbalances between the I and Q branches result in finite and usually insufficient rejection of the image tone [5][6]. In addition, practical mixers always leak part of the LO signals into their output ports, generating another undesired tone to the synthesized signal. To compensate for these non-idealities, the idea here is to use digital pre-distortion of the low frequency tone as presented in Figure 1.

This work was carried out in the project "Digital and Analog Techniques for Flexible Receivers" funded by the National Technology Agency of Finland (Tekes). The work was also supported by the Academy of Finland, the Graduate School in Electronics, Telecommunications and Automation (GETA), and the Spanish Government (CICYT) TIC 2001-2481.

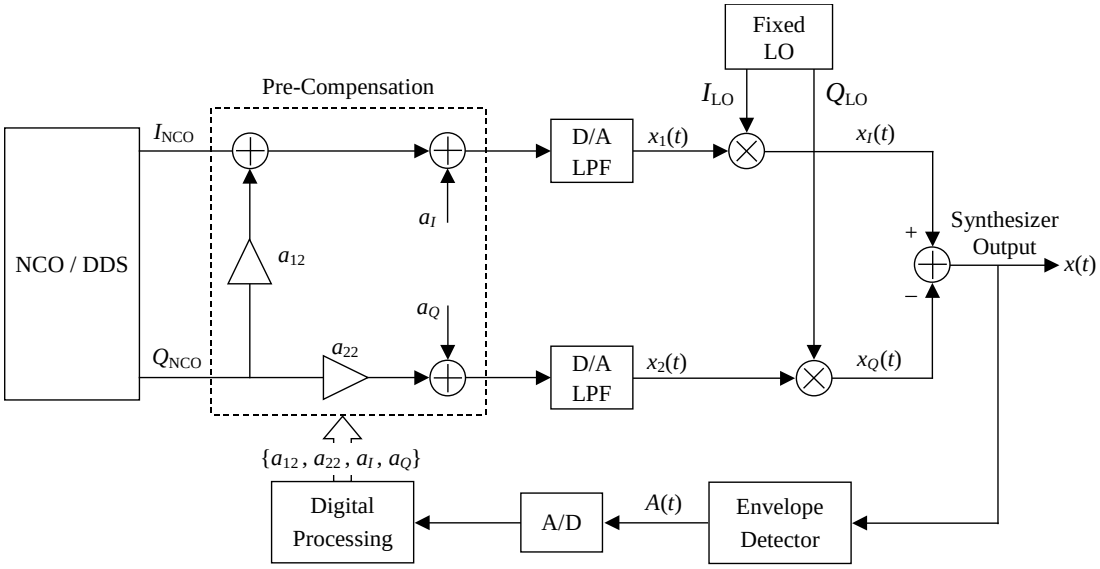

Figure 1. Synthesizer architecture where digital pre-compensation is used to compensate for the non-idealities of the analog part.

3. SIGNAL ANALYSIS

3.1 I/Q Imbalance, LO leakage, and Pre-Compensation

Our signal modeling builds on the ideas reported in [7]. In this contribution, an expression for the synthesizer output signal is derived assuming both carrier leakage and I/Q imbalance. Without loss of generality, we write the low frequency I and Q signals in continuous-time domain as $I_{NCO}(t) = \cos(\omega_{NCO}t)$ and $Q_{NCO}(t) = \sin(\omega_{NCO}t)$. Similarly, the I/Q mixer LO signals are defined here as $I_{LO}(t) = \cos(\omega_{LO}t)$ and $Q_{LO}(t) = g\sin(\omega_{LO}t + \phi)$ where g and ϕ represent the gain and phase imbalances, respectively. Notice that introducing the imbalances only in the Q branch of the mixer LO signal is a valid model since what matters is only the relative difference between the I and Q branches. Also any gain mismatch between the I and Q branch D/A converters and filters can be modeled in the mixer gain imbalance g. Previous work demonstrates that if the motivation is just to remove the image tone, simple pre-compensation scheme with two coefficients a_{12} and a_{22} is sufficient [7]. In addition to the image tone compensation, two additional coefficients a_I and a_Q are employed here to compensate for the carrier leakage effect as well.

Referring to the model in Figure 1, the output signals $x_I(t) = [x_1(t) + L_I]\times I_{LO}(t)$ and $x_Q(t) = [x_2(t) + L_Q]\times Q_{LO}(t)$ of the two mixers are given by

$$x_I(t) = [a_I + L_I + \cos(\omega_{NCO}t + \theta_1) + a_{12}\sin(\omega_{NCO}t + \theta_1)]\times\cos(\omega_{LO}t)$$
$$x_Q(t) = [a_Q + L_Q + a_{22}\sin(\omega_{NCO}t + \theta_2)]\times g\sin(\omega_{LO}t + \phi) \quad (1)$$

where θ_1 and θ_2 model the relative phase shift due to the D/A converters and branch filters and L_I and L_Q model the carrier leakage of the I and Q mixers, respectively. Then, the synthesizer output signal $x(t) = x_I(t) - x_Q(t)$ can be expressed as $x(t) = \mathrm{Re}[x_{LP}(t)\exp(j\omega_{LO}t)]$ where the lowpass equivalent $x_{LP}(t)$ is given by

$$x_{LP}(t) = \alpha e^{j\omega_{NCO}t} + \beta e^{-j\omega_{NCO}t} + \gamma\,. \quad (2)$$

In other words, the output signal $x(t)$ consists of three frequency components: the desired component $\omega_{LO} + \omega_{NCO}$, the image component $\omega_{LO} - \omega_{NCO}$ and the carrier leakage component ω_{LO}. The relative strengths of these spectral components are α, β and γ, which in turn depend on g, ϕ, $\theta = \theta_2 - \theta_1$, L_I and L_Q as well as on the compensation parameters a_{12}, a_{22}, a_I and a_Q. In practical implementations, the image tone attenuation defined here as

$$L_{IMAGE} = |\alpha|^2 \,/\, |\beta|^2 \quad (3)$$

is only 20 … 40 dB if no compensation is used (i.e., $a_{12} = 0$ and $a_{22} = 1$). Similarly, the carrier tone attenuation defined as

$$L_{CARRIER} = |\alpha|^2 \,/\, |\gamma|^2 \quad (4)$$

can commonly range around 30 … 40 dB without compensation.

Practical implementations require image and carrier leakage attenuations around 60 … 80 dB [4]. Ideally, with proper values of pre-compensation coefficients a_{12}, a_{22}, a_I and a_Q, the image and carrier tones can be completely removed from the synthesizer output. In our notation, this simply corresponds to pre-compensation parameters for which $\beta = \gamma = 0$ (while $|\alpha| \neq 0$ of course). It can be shown that one solution to achieve this is to set

$$a_{12} = \tan(\psi)\,,\ a_{22} = \frac{1}{g\cos(\psi)}\,,\ a_I = -L_I\,,\ a_Q = -L_Q \quad (5)$$

where $\psi = \phi - \theta$. Notice that the pre-compensation parameters can be gathered into two independent groups: a_{12}, a_{22} related to image tone compensation and a_I, a_Q related to carrier leakage compensation.

3.2 Iterative Coefficient Update

In practice, in order to calculate the pre-compensation coefficients of (5), the unknown non-idealities need to be estimated or measured somehow. With simple implementation in mind, the approach here is to estimate the parameters iteratively using only the envelope

$$A(t) = |x_{LP}(t)| = \Big(|\alpha|^2 + |\beta|^2 + |\gamma|^2 + 2\,\mathrm{Re}[\alpha\beta^* e^{j2\omega_{NCO}t}] + 2\,\mathrm{Re}[(\alpha\gamma^* + \gamma\beta^*)e^{j\omega_{NCO}t}]\Big)^{1/2} \quad (6)$$

of the synthesized signal. With the solution given in (5), $\beta = \gamma = 0$ causing the output envelope to be flat (i.e., $A(t) = |\alpha|$) as expected.

Instead of estimating the actual non-idealities, which would then be used in (5), an alternative approach is to directly adapt a_{12}, a_{22}, a_I and a_Q in an iterative manner to minimize the envelope variation. See [8] and [9] for related discussions on I/Q data modulators. Considering the relation in (6) between the output envelope and the compensation parameters, several different approaches to monitor the envelope behaviour can be envisioned. One interesting yet simple (ad-hoc) possibility is to consider the envelope peak-to-peak (PP) value

$$d_A = \max\{A(t)\} - \min\{A(t)\} \,. \tag{7}$$

Clearly, d_A is zero if the envelope is flat.

According to the preliminary results, the principal behavior of d_A as a function of a_{12} and a_{22} is only slightly dependent on the relative carrier leakage values. As shown in Figure 2, the d_A -surface when viewed as a function of a_{12} and a_{22} has a unique minimum located at $a_{12} = \tan(\psi)$ and $a_{22} = 1/(g\cos(\psi))$. Similarly, I/Q imbalance has only a small effect on d_A when examined as a function of a_I and a_Q. As depicted in Figure 3, the d_A -surface explored as a function of a_I and a_Q has a unique minimum as well, at $a_I = -L_I$ and $a_Q = -L_Q$. Based on these observations, the d_A -surface lends itself well to iterative minimization.

The true gradient of d_A (derivative with respect to a_{12}, a_{22}, a_I and a_Q) depends on g, ψ, L_I and L_Q which are unknown in practice. One practical approach is to adapt only one of the four parameters at a time and freeze the others. In this case, the direction (here sign) of the needed one-dimensional gradient at each iteration can be determined according to the behavior of d_A between two consecutive adaptations of the corresponding parameter. This leads to the following update rule:

$$a_I(n) = a_I(n-4) + K_I(n)\lambda_1 \frac{d_A(n)}{d_A(n) + \lambda_2} \tag{8a}$$

for n = 1, 5, 9, …, with $K_I \in \{+1, -1\}$,

$$a_Q(n) = a_Q(n-4) + K_Q(n)\lambda_1 \frac{d_A(n)}{d_A(n) + \lambda_2} \tag{8b}$$

for n = 2, 6, 10, …, with $K_Q \in \{+1, -1\}$,

$$a_{12}(n) = a_{12}(n-4) + K_{12}(n)\lambda_1 \frac{d_A(n)}{d_A(n) + \lambda_2} \tag{8c}$$

for n = 3, 7, 11, …, with $K_{12} \in \{+1, -1\}$ and

$$a_{22}(n) = a_{22}(n-4) + K_{22}(n)\lambda_1 \frac{d_A(n)}{d_A(n) + \lambda_2} \tag{8d}$$

for n = 4, 8, 12, …, with $K_{22} \in \{+1, -1\}$. In the above update equations, the value of the update sign $K_I(n)$ is either $+K_I(n-4)$ or $-K_I(n-4)$ depending on whether the last update of a_I caused the envelope variation d_A to decrease or increase. Similar reasoning is used for the other update signs K_Q, K_{12} and K_{22}. Depending on the feasible range of each parameter, the values for the adaptation step-sizes $\lambda_1 > 0$ and $\lambda_2 \geq 0$ can and should be selected individually. Notice that the magnitude of the update term is anyway always bounded to be between zero and λ_1. With very large values of d_A, the amount of update is close to λ_1 while small values of d_A cause only a small change to the parameter at hand.

4. EXAMPLE SIMULATIONS

Some computer simulations are carried out to demonstrate the performance of the proposed frequency synthesizer concept. For illustration purposes, realistic I/Q imbalance values of $g = 1.04$, $\theta = 1°$ and $\phi = 6°$ ($\psi = 5°$) and carrier leakage levels of $L_I = -40$ dB and $L_Q = -35$ dB are used, corresponding to image and carrier tone attenuations of approximately 26 dB and 34 dB, respectively. After initializing the pre-compensation coefficients as $a_I = 0$, $a_Q = 0$, $a_{12} = 0$, and $a_{22} = 1$, they are iteratively updated one-by-one to minimize the peak envelope variation according to (8a)-(8d). In the basic simulations, one adaptation is performed per envelope period and, for the sake of simplicity, identical step-size values of $\lambda_1 = 0.02$ and $\lambda_2 = 0.05$ are used for both a_{12} and a_{22}, and $\lambda_1 = 0.002$ and $\lambda_2 = 0.01$ for both a_I and a_Q.

With these simulation values, the d_A -surface is illustrated as a function of a_{12} and a_{22} in Figure 2, and as a function of a_I and a_Q in Figure 3. In the a_{12}-a_{22} and a_I-a_Q -planes, the convergence of the corresponding pre-compensation coefficients during one simulation realization is presented. The behavior of the synthesized output envelope is depicted in Figure 4 demonstrating successful synthesizer operation. With the given non-idealities and step-size parameters, the steady-state operation is reached in 50 iterations or so and in general image and carrier tone attenuations in the order of 100-150 dB are theoretically feasible.

To demonstrate the correct operation of the synthesizer also in time-varying environments, a rapid change in the non-idealities is caused and the tracking capability of the pre-compensation scheme is verified. From the practical point of view, these non-idealities are not expected to vary strongly as a function of time if the operating frequency is kept constant. Some slight drifting can be caused though by temperature changes or device ageing, for example. On the other hand, when the operating frequency is changed, also the leakage and especially imbalance properties are likely to change, e.g., due to frequency dependent differences in the filter frequency responses. The gain imbalance g is here changed from 1.04 to 0.98, the phase imbalance ϕ from 6° to 3° (new $\psi = 2°$), and the new carrier leakage levels are $L_I = -40$ dB and $L_Q = -40$ dB. With these changes, the resulting output envelope is depicted in Figure 5. Clearly, the compensator responds quickly to the changes and adapts the coefficients accordingly.

5. IMPLEMENTATION ASPECTS

In the proposed synthesizer concept, both I/Q imbalance and carrier leakage compensation are carried out at the same stage. Modeling also the effect of LO leakage, according to the expression given by (6), the envelope of the synthesizer output signal is periodic with fundamental frequency ω_{NCO}. Thus, assuming that d_A is determined and pre-compensation parameters are updated once per envelope cycle (or once per several cycles), careful frequency planning is needed to reach a reasonable compromise between convergence speed and power consumption. In other words, the minimum frequency synthesized in the digital part should be selected in such a manner that the envelope variation rate does not limit the achievable settling time. Higher frequencies in the digital part, in turn, always imply higher sampling and clock rates and, thus, higher power consumption.

Also of vital importance in any digital system is the number of bits needed in internal calculations and to represent the data. The required pre-compensation coefficient word-length depends on the target image and carrier tone levels after convergence. Preliminary

analysis of these issues has shown that image and carrier tone attenuations in the order of 80 dB are achievable even with 12 bits. However, further and more detailed studies related to this matter are still needed. Notice that in general information about the reasonable range of the pre-compensation coefficients can be utilized to optimize their digital implementation. Also in time- and/or frequency hopping systems, the previous values of the compensation parameters can be used for initialization.

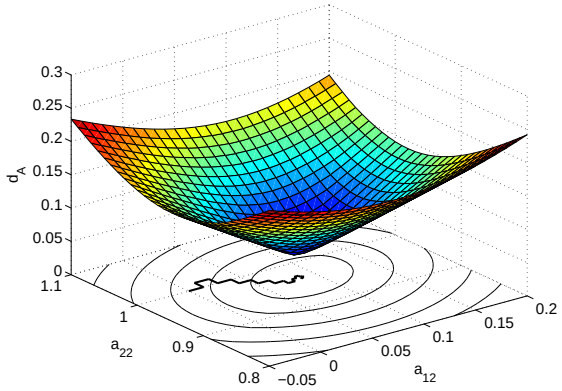

Figure 2. Envelope peak-to-peak value d_A as a function of the compensation parameters a_{12} and a_{22} (with $a_I = 0$, $a_Q = 0$) for $g = 1.04$, $\psi = 5°$, $L_I = -40$ dB and $L_Q = -35$ dB. Also shown in the a_{12}-a_{22} -plane is one realization of the compensation parameters during the adaptation.

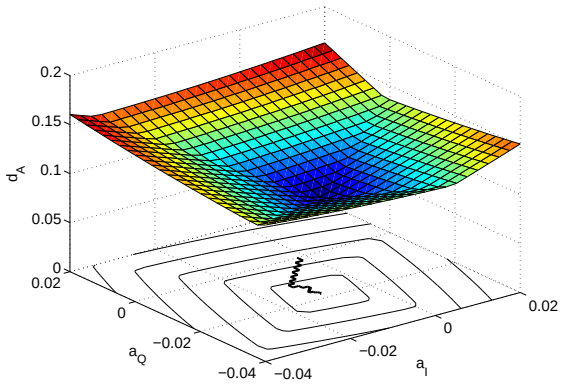

Figure 3. Envelope peak-to-peak value d_A as a function of the compensation parameters a_I and a_Q (with $a_{12} = 0$, $a_{22} = 1$) for $g = 1.04$, $\psi = 5°$, $L_I = -40$ dB and $L_Q = -35$ dB. Also shown in the a_I-a_Q -plane is one realization of the compensation parameters during the adaptation.

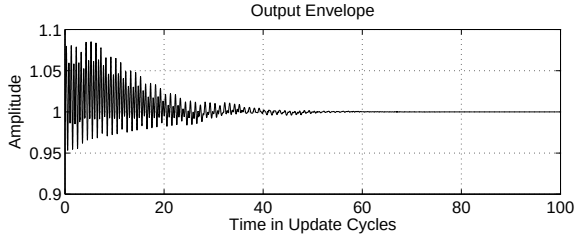

Figure 4. Envelope of the synthesizer output signal during the adaptation for $g = 1.04$, $\psi = 5°$, $L_I = -40$ dB and $L_Q = -35$ dB.

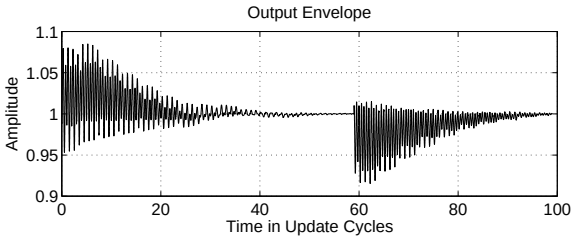

Figure 5. Envelope of the synthesizer output signal during the adaptation with a rapid change in the non-idealities. The initial values $g = 1.04$, $\psi = 5°$, $L_I = -40$ dB and $L_Q = -35$ dB are changed to $g = 0.98$, $\psi = 2°$, $L_I = -40$ dB and $L_Q = -40$ dB, respectively.

6. CONCLUSIONS

In wireless applications, the design of frequency synthesizers is a challenging task. To achieve fast switching capabilities and high operating frequencies with reasonable power consumption, a frequency synthesizer based on digital tuning and I/Q mixing has been presented. From an implementation point of view, I/Q mismatch and carrier leakage are important issues to consider and their effects were analyzed in detail. Based on this analysis, a pre-compensation scheme was formulated which ideally provides complete carrier and image tone rejection. A simple iterative algorithm was also presented to determine the compensator coefficients in an efficient manner. The proper operation of the frequency synthesizer was demonstrated through computer simulations, both in static and time-varying situations. Future work should be directed to hardware prototyping and/or co-simulation of the analog and digital parts in order to assess the practical performance of the proposed synthesizer.

7. REFERENCES

[1] U. L. Rohde, *Microwave and Wireless Synthesizers: Theory and Design*. New York: John Wiley & Sons, 1997.

[2] J. Craninckx and M. Steyaert, *Wireless CMOS Frequency Synthesizer Design*. Dordrecht, The Netherlands: Kluwer Academic Publishers, 1998.

[3] V. F. Kroupa, Ed., *Direct Digital Frequency Synthesizers*. Piscataway, NJ: IEEE Press, 1999.

[4] B. Razavi, "Challenges in the design of frequency synthesizers for wireless applications," in *Proc. IEEE Custom Integrated Circuits Conf.*, Santa Clara, CA, May 1997, pp. 395-402.

[5] C. Chien, *Digital Radio Systems on a Chip*. Norwell, MA: Kluwer Academic Publishers, 2001.

[6] M. Valkama, M. Renfors, and V. Koivunen, "Advanced methods for I/Q imbalance compensation in communication receivers," *IEEE Trans. Signal Processing*, vol. 49, pp. 2335-2344, Oct. 2001.

[7] C. Caballero Gaudes *et al.*, "Fast frequency synthesizer concept based on digital tuning and I/Q signal processing," in *Proc. IEEE Int. Conf. Digital Signal Processing*, Santorini, Greece, July 2002, pp. 1317-1320.

[8] M. Faulkner, T. Mattsson, and W. Yates, "Automatic adjustment of quadrature modulators," *Electron. Lett.*, vol. 27, pp. 214-216, Jan. 1991.

[9] R. Marchesani, "Digital precompensation of imperfections in quadrature modulators," *IEEE Trans. Commun.*, vol. 48, pp. 552-556, Apr. 2000.